# Insights into $H_2$ formation in space from ab initio molecular dynamics

Simone Casolo[a], Gian Franco Tantardini[a,b], and Rocco Martinazzo[a,b,1]

[a]Dipartimento di Chimica, Università degli Studi di Milano, 20133 Milan, Italy; and [b]Consiglio Nazionale delle Ricerche–Istituto di Scienze e Tecnologie Molecolari, 20133 Milan, Italy

Edited by Donald G. Truhlar, University of Minnesota, Minneapolis, MN, and approved March 12, 2013 (received for review January 25, 2013)

**Hydrogen formation is a key process for the physics and the chemistry of interstellar clouds. Molecular hydrogen is believed to form on the carbonaceous surface of dust grains, and several mechanisms have been invoked to explain its abundance in different regions of space, from cold interstellar clouds to warm photon-dominated regions. Here, we investigate direct (Eley–Rideal) recombination including lattice dynamics, surface corrugation, and competing H-dimers formation by means of ab initio molecular dynamics. We find that Eley–Rideal reaction dominates at energies relevant for the interstellar medium and alone may explain observations if the possibility of facile sticking at special sites (edges, point defects, etc.) on the surface of the dust grains is taken into account.**

graphite–graphene | interstellar chemistry | hydrogen recombination | density functional theory

The complicated interaction between hydrogen atoms and graphite has been widely studied in the last decade because of its relevance in various fields, from hydrogen storage (1) to nuclear fusion (2), from graphene technology (3–6) to interstellar chemistry (7).

In the chemistry of the interstellar medium (ISM), $H_2$ is a precursor for more complex molecules through its protonated form $H_3^+$, shields the clouds from the radiation field, and acts as primary cooling agent during the gravitational collapse, which ultimately leads to star formation (7). Its appearance in the early universe steered the development of the first stars and triggered galaxy formation (8).

In the harsh ISM conditions, molecular hydrogen is continuously dissociated by stellar UV radiation and cosmic rays; hence efficient synthetic pathways are needed to explain the observed abundances (7). These are known to involve the carbonaceous surface of interstellar dust grains (9), but the detailed mechanisms behind $H_2$ formation on graphitic surfaces have yet to be fully uncovered.

Physisorbed H atoms can only be invoked in cold molecular clouds, where the surface temperature is low enough to prevent desorption ($T_s \lesssim 40$ K) from the shallow physisorption well ($E \sim 4$ kJ·mol$^{-1}$) (10, 11). In this case, hydrogen molecules may follow from either an Eley–Rideal (ER)/hot-atom (HA) or a Langmuir–Hinshelwood (LH) pathway, because H atoms are very mobile even at extremely low temperatures (11). Stable (chemisorbed) species on the basal graphitic plane, however, require energetic projectile atoms to overcome an activation barrier to sticking ($E \sim 20$ kJ·mol$^{-1}$) (12, 13), which is due to the carbon $sp^2$–$sp^3$ rehybridization needed by the bond formation process, although tunneling might help in this context (14). Chemically bound H atoms are immobile on the surface [they desorb rather than diffusing (15)]; hence LH pathway is ruled out in sufficiently warm environments where only chemisorbed species can be found.

No matter how a first chemisorbed species is formed, secondary H atoms undergo facile sticking and preferentially form *ortho* and *para* (16, 17) dimers because of the aromatic nature of the surface (18), analogously to the *ortho–para* orientation effect in electrophilic aromatic substitution reactions. Hence, ER/HA recombination competes with dimer formation (DF), and may occur on isolated H atoms as well as on dimers (or clusters) of adsorbates [recombination can also directly occur from *o*- and *p*- dimers if the surface is heated up (15)]. In the latter case, a catalytic cycle could be envisaged (16, 19) if DF were much more favored than direct ER recombination. Otherwise, ER reaction would remove the "active" H atom, and a further (likely activated) adsorption event would be needed to start a new molecular formation process.

At present, experimental evidence about the ER reaction and the competing DF is scarce, and often limited to the high energy regime required for the first-H adsorption event to occur. With the same token, theoretical modeling has been mainly hampered by the knowledge of the interaction potential, and often limited to reduced dynamical models where a full quantum dynamical approach could be applied. For this reason, theoretical results for the above ER recombination have been so far considered of limited help and never used in modeling the chemistry of the ISM.

In this article, we use ab initio molecular dynamics (AIMD) to investigate the (barrierless) ER reaction and the formation of H dimers on a graphite surface. We consider a H atom impinging on a graphene layer (initially at $T_s = 0$ K) containing a chemisorbed H, and follow classical trajectories of motion by using first principles [density functional theory (DFT)] forces computed on-the-fly as required by the dynamics itself. In this way, we are able to include all of the relevant degrees of freedom at the DFT electronic structure level, at a price of using classical mechanics for the molecular dynamics. We then correct a posteriori for quantum effects at low collision energies, where we rely on recent quantum results obtained on a realistic reduced dynamical model (20). We are thus able to provide reliable data (rate constants) for the ER $H_2$ formation on graphite on a wide temperature range and to determine effective recombination rates for hydrogen formation in the ISM, which can be directly compared with astronomical observations.

## Results and Discussion

Computed ER and DF cross-sections are shown in Fig. 1*A* in the collision energy ($E_{coll}$) range from 2 to 100 kJ·mol$^{-1}$ for the ground (singlet) adiabatic state of the overall system, corrected for the proper 1/4 spin-statistical factor. Overall, abstraction cross-sections are quite large (3.5 Å$^2$), much larger than those found for hydrogen on metals, ≤1 Å$^2$, in agreement with previous studies (21, 22). They decrease when increasing the collision energy because of the competing sticking of the projectile atom (DF). For the latter process, the cross-section is indeed remarkably high, with a maximum of ∼7.5 Å$^2$ at $E_{coll}$ of ∼80 kJ·mol$^{-1}$, in qualitative agreement with scanning tunneling microscopy

Author contributions: G.F.T. and R.M. designed research; S.C. and R.M. performed research; G.F.T. contributed fundings and resources; S.C. and R.M. analyzed data; and S.C. and R.M. wrote the paper.

The authors declare no conflict of interest.

This article is a PNAS Direct Submission.

[1]To whom correspondence should be addressed. E-mail: rocco.martinazzo@unimi.it.

This article contains supporting information online at www.pnas.org/lookup/suppl/doi:10.1073/pnas.1301433110/-/DCSupplemental.

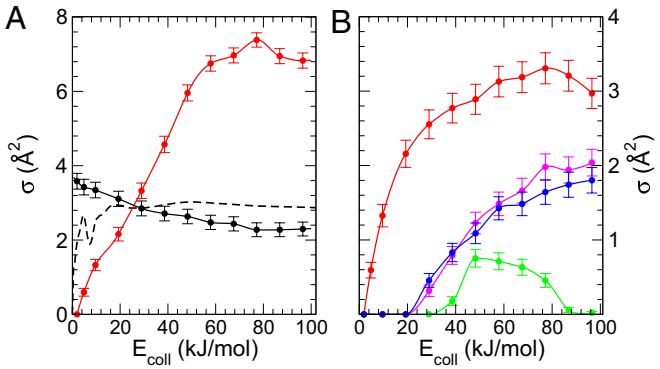


**Fig. 1.** (*A*) Cross-sections for ER recombination (black) from classical AIMD (full line) and quantum calculations on a reduced model (from ref. 20) (dashed). DF from AIMD are also shown (red line). Error bars give estimated statistical errors. (*B*) Cross sections for *ortho* (blue), *meta* (green), and *para* (red) dimers and for the sum of the remaining dimer structures (magenta).

observations, which showed that the dimer abundance exceeds well the predictions of random adsorption models (16, 17).

Details of DFs are reported in Fig.1*B* where the preference toward *ortho* and *para* DF is made evident. The preferential formation of "balanced" dimers (with H sitting on opposite graphenic sublattices) is a consequence of the (almost) barrierless path to sticking when the projectile H couples favorably with the itinerant electron set free by the first adsorption event (16, 18). *Para*-dimers (whose formation is truly barrierless) are the most abundant ones, and their abundance can be as high as one-half the total dimer fraction. Despite this, *para* DF shows a dynamical threshold of about 2 kJ·mol$^{-1}$ (corresponding to a gas-phase temperature $T_g \sim 300$ K), below which only $H_2$ recombination is expected. This is in agreement with recent experiments, in which highly oriented pyrolitic graphite (HOPG) samples precovered with D atoms were found to form dimers and clusters only when irradiated with highly energetic H atoms (23); at $E_{coll}$ = 2.4 kJ·mol$^{-1}$, only ER recombination was found to occur (24). More generally, as is evident in Fig. 1*A*, ER abstraction dominates at collision energies smaller than $\sim$20 kJ·mol$^{-1}$, thereby suggesting that no catalytic cycle involving dimers can be operative in usual interstellar cloud conditions ($T_g$ = 1–1,000 K).

AIMD results for ER reaction can be compared with "effective" abstraction cross-sections available from kinetic measurements using $\sim$20 kJ·mol$^{-1}$ H beams on D-precovered HOPG samples at a surface temperature $T_s$ = 150 K (25). Modeling the kinetic data cannot distinguish ER from HA contributions for hot species with a preference for reaction over sticking (26). The latter are expected to be active at low $T_s$ and low coverage, and indeed such effective cross-section levels off at high coverage and reaches a value of $\sim$3.5 Å$^2$ (25). This in good agreement with our computed value $\sigma = 3.1 \pm 0.2$ Å$^2$ at 20 kJ·mol$^{-1}$.

We also determined rovibrational populations of the nascent molecules and tentatively compared them with available experimental data (27–29) obtained with cold atomic beams ($T_g$ = 300 K) on cold HOPG surfaces ($T_s$ = 15 K). These latter results, apparently relevant for the physisorption regime only (see below), seem to be compatible with ER processes because recent theoretical studies on LH/HA recombination of physisorbed species have predicted $H_2$ molecules with a much larger rotational excitation than found in the experiment (30–32). In this case, a comparison is reasonable on the basis of a common reaction mechanism, although a different energetics might play a role in determining the details. Surprisingly, the result of such a comparison (Fig. 2) is remarkably good and supports the idea that ER recombination dominates under these conditions too.

On comparing at medium-to-high $E_{coll}$, the AIMD reaction cross-sections with numerically exact, quantum mechanical (QM) results obtained within the rigid, flat surface approximation (33), we can assess the influence of surface corrugation. In this energy regime, quantum and classical results agree to each other to within $\sim$0.5 Å$^2$ (Fig. 1), thereby substantially validating previous studies (13, 22, 33), which could not take into account surface corrugation, DF, and lattice relaxation. At low energies, two competing effects lead to a marked discrepancy between the two sets of data. On the one hand, quantum calculations correctly describe the effect of increasing the de Broglie wavelength of the projectile atom at decreasing energies, e.g., the quantum reflection off a potential well, by predicting a vanishing cross-section in the limit of vanishing energy (20). On the other hand, again because of the limitations of a reduced dynamical model, quantum calculations could not take into account any steering effect arising from the presence of attractive sites close to the reaction center. This steering effect is clearly present in the classical results, which show an increasing cross-section at low energy. Detailed analysis of the trajectories shows that this effect is due to the active role played by the *para* positions in redirecting projectile atoms toward the target (*Supporting Information*, *Projectile Steering*). A similar *para*-mediated abstraction has been recently postulated and used in kinetic Monte Carlo simulations of hydrogen abstraction of graphitic surfaces (34).

In view of the above, we performed a weighted average of the AIMD and QM cross-sections, and computed thermal rate constants for the ER reaction in the range $T_g$ = 20–1,000 K (see

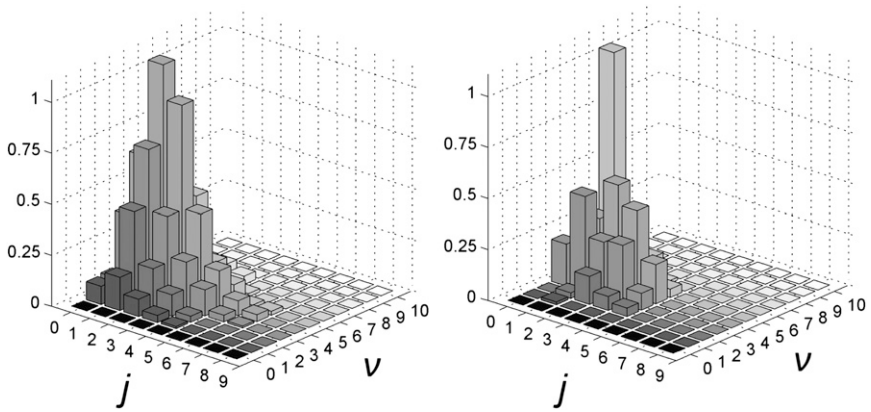


**Fig. 2.** Relative populations of HD product rovibrational states. (*Left*) Experimental data taken from ref. 29. (*Right*) AIMD results for HD formed in collisions of H atoms with chemisorbed D.

*Supporting Information*, *Reaction Rates* for details). Finally, we set up a minimal kinetic model including sticking, reaction, and desorption, and used the above-computed rate constants to write the hydrogen formation rate as follows:

$$\frac{dn_v^{H_2}}{dt} \simeq \frac{k_s k_{ER}}{k_s \Sigma_s + k_{ER}} \Sigma_g n_v^g n_v^H = R n n_v^H . \quad [1]$$

Here, $n_v^X$ is the number of $X$ per unit volume ($X = H, H_2$, and $g$ for H atoms, $H_2$ molecules, and dust grains), $\Sigma_g$ and $\Sigma_s$ are the average surface area per grain and per site, respectively, and $k_{ER}$ and $k_s$ are the ER and sticking rate constants. The latter involves an average of the sticking probability ($P_s$) over the velocity of the incoming projectiles, namely $k_s = \langle P_s v_z \rangle$, and thus the term $k_s \Sigma_s$ in the denominator contains the sticking cross-section $\sigma_s = P_s \Sigma_s$. Finally, $n$ is the total hydrogen concentration and $R$ is an effective recombination rate (see *Supporting Information*, *Kinetic Model* for details of the model).

The results for representative values of the (unknown) initial sticking coefficient $P_s$ are shown in Fig. 3 for model spherical grains with average radius 170 nm and density $n_v^g = 4 \times 10^{-13} n$, together with recombination rates inferred from astronomical observations (35, 36). It is clear from the figure that the minimal model including only ER recombination out of chemisorbed species does account for the observations, but only if an unusually large (initial) sticking coefficient is assumed ($P_s \sim 1$). The latter is not compatible with the activated adsorption of H atoms on the basal plane of a graphitic surface. Reaction between physisorbed species could account for the observation (the grain surface temperature is always much lower than $T_g$), but sticking might be an issue in this case too, because recent accurate QM calculations estimated $P_s \sim 0.01$ under these conditions (37). Moreover, physisorbed species can only be invoked in cold environments, and thus different mechanisms would be required to explain hydrogen formation in warm regions of space, e.g., photon-dominated regions.

Fortunately, there is no real need to invoke different scenarios. Facile chemisorption is possible at special sites—for instance, at the edges, at the grain boundaries, or close to a point defect—where a sticking cross-section as large as $\sim 20$ Å$^2$ can be expected. In such instances, direct chemisorption is possible because barrierless paths exist for adsorption at these sites (38). Also, physisorbed species would contribute at low surface temperature (raising the sticking cross-section) because they move easily on the surface, no matter how small $T_s$ is, until they get trapped in the above special sites by formation of strong chemical bonds. In conjunction with ER recombination, this would provide a general route to $H_2$, which applies to warm as well as cold environments, with at most a "temperature-dependent" effective sticking cross-section. The red curve in Fig. 3, for instance, shows the effect of active sites in a realistic porous grain model, with a grain surface area 50 times larger than the one used above for spherical grains, a defect density of $1.5 \times 10^{-2}$ per carbon atom and a sticking cross-section of 17.8 Å$^2$ (see *Supporting Information*, *Kinetic Model* for details).

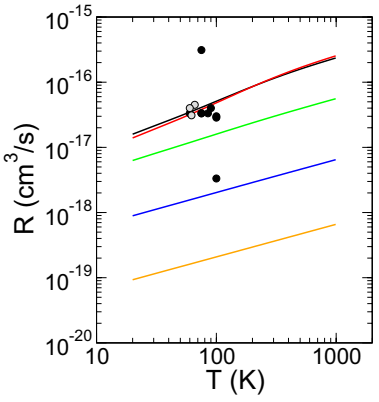


**Fig. 3.** Total effective $H_2$ recombination rates obtained for different H atom sticking coefficients ($P_s = 10^{-n}$ with $n = 0-3$ in black, green, blue, and orange, respectively), for a simple spherical grain model. Also shown in red the results for a more realistic, porous grain model including active sites with a sticking cross-section of about $\sim 20$ Å$^2$. Data from astronomical observation are shown as dark (35) and light (36) dots.

## Conclusions

We have investigated hydrogen formation in the ISM by focusing on the direct ER recombination and the competing process forming dimers on graphite. With the help of ab initio molecular dynamics simulations, we included lattice dynamics, surface corrugation, and the possibility of forming dimers, and established that dimers cannot play any role in the hydrogen formation at ISM conditions. Rather, we find that ER reaction involving stable (chemisorbed) species is efficient enough to explain alone $H_2$ abundances under different conditions, provided the possibility of facile sticking at special sites is considered.

## Materials and Methods

AIMD simulations were performed with the VASP package (39). Exchange and correlation were considered following the PW91 (40) functional. The plane wave basis set was limited to a 300-eV cutoff, for valence electrons, whereas the atomic cores were described by ultrasoft pseudopotentials (41). To simulate the graphite surface, we used a H atom in a 3 × 3 graphene layer, corresponding to a 1/18 ML coverage, with atoms at their (optimized) equilibrium positions. The Brillouin zone was integrated on a 3 × 3 × 1 Γ-centered $k$ points mesh. This setup was carefully tested for the case of a single H atom chemisorbed on graphene, to give an error smaller than 20 meV (1.93 kJ·mol$^{-1}$) on the binding energies, 10 meV (0.96 kJ·mol$^{-1}$) on barriers and of about 0.04 Å on the bond lengths as computed in ref. 18. These error estimates are consistent with those found in evaluating and fitting the potential energy surfaces used for quantum time dependent wave packet calculations (21).

Dynamical simulations were performed sampling the microcanonical ensemble with classical trajectories. Hellmann–Feynman forces were computed on-the-fly with DFT while the Newton equations of motion were integrated using a Verlet algorithm, as implemented in VASP, with a 0.40-fs time step. Carbon and target H atoms were initially kept at rest, implying $T_s = 0$ K, and left free to move during the whole simulation; ER reaction is expected to be little influenced by the surface temperature [even when vibrational excitation of the target occurs (22, 42)], and thus this $T_s$ value is expected to be appropriate for ISM conditions ($T_s$ = 5–100 K). Only the height of one of the carbon atoms furthest away from the target was kept fixed to prevent block translation of the whole system. Initial surface atom positions were determined by a geometry optimization run using a 0.01 eV/Å threshold on each atomic force.

A monochromatic beam of H atoms was simulated by placing projectile atoms at 5 Å from the graphite surface with a velocity directed toward the surface at normal incidence. Aiming points were generated by a uniform Monte Carlo sampling of an irreducible area ($\theta = \pi/3$, $r$ = 3.55 Å) centered on the target H atom. For each collision energy, we run 500 trajectories, equivalent to 3,000 trajectories on the whole circular area surrounding the projectile. The number of trajectories was increased to 1,000 (per irreducible area) when computing rovibrational populations at selected energies. The spins of the H projectile and that of the hydrogenated surface were initially set antiparallel to mimic a singlet state, and then cross-sections were scaled by a factor of 1/4 to account for the (nonreactive) triplet manifold.

The reactive channels considered in the molecular dynamics simulations were the ER recombination, DF, and collision-induced desorption. For the recombination channel, each product molecule was assigned to a rotational and vibrational state, based on standard binning into the rovibrational spectrum of the $H_2$ (HD) molecule, as obtained with the help of a standard Colbert–Miller discrete variable representation Hamiltonian (43). Dimers formation was considered on every carbon atom lying not further than 4 $d_{C-C}$. In agreement with previous studies (22), no collision-induced desorption was found in the collision energy range considered.

Further details on the rate constant calculations and on the kinetic model can be found in *Supporting Information*, *Reaction Rates* and *Kinetic Model*.

**ACKNOWLEDGMENTS.** We acknowledge T. Zecho and H. Cuppen for useful discussions. S.C. thanks G.-J. Kroes for the hospitality during his stay in Leiden Universiteit, where a preliminary stage of this work was conducted. This work has been supported by Regione Lombardia and Consorzio Interuniversitario Lombardo per l'Elaborazione Automatica consortium (CILEA) through a Laboratory for Interdisciplinary Advanced Simulation (LISA) Initiative (2010) grant.

1. Psofogiannakis GM, Froudakis GE (2011) Fundamental studies and perceptions on the spillover mechanism for hydrogen storage. *Chem Commun (Camb)* 47(28):7933–7943.
2. Küppers J (1995) The hydrogen surface chemistry of carbon as plasma facing material. *Surf Sci Rep* 22(7–8):249–322.
3. Elias DC, et al. (2009) Control of graphene's properties by reversible hydrogenation: Evidence for graphane. *Science* 323(5914):610–613.
4. Bostwick A, et al. (2009) Quasiparticle transformation during a metal-insulator transition in graphene. *Phys Rev Lett* 103(5):056404.
5. Balog R, et al. (2010) Bandgap opening in graphene induced by patterned hydrogen adsorption. *Nat Mater* 9(4):315–319.
6. Haberer D, et al. (2010) Tunable band gap in hydrogenated quasi-free-standing graphene. *Nano Lett* 10(9):3360–3366.
7. Wakelam V, et al. (2010) Reaction networks for interstellar chemical modelling: Improvements and challenges. *Space Sci Rev* 156:13–72.
8. Schlemmer S (2011) H2 generation in the early universe governs the formation of the first stars. *Angew Chem Int Ed* 50(10):2214–2215.
9. Hollenbach DJ, Salpeter EE (1971) Surface recombination of hydrogen molecules. *Astrophys J* 163:155–164.
10. Ghio E, Mattera L, Salvo C, Tommasini F, Valbusa U (1980) Vibrational spectrum of H and D on the (0001) graphite surface from scattering experiment. *J Chem Phys* 73(1): 556–562.
11. Bonfanti M, Martinazzo R, Tantardini GF, Ponti A (2007) Physisorption and diffusion of hydrogen atoms on graphite from correlated calculations on the H-coronene model system. *J Phys Chem C* 111(16):5825–5829.
12. Jeloaica L, Sidis V (1999) DFT investigation of the adsorption of atomic hydrogen on a cluster-model graphite surface. *Chem Phys Lett* 300(1–2):157–162.
13. Sha X, Jackson B (2002) First-principles study of the structural and energetic properties of H atoms on a graphite (0001) surface. *Surf Sci* 496(3):318–330.
14. Goumans TPM, Kästner J (2010) Hydrogen-atom tunneling could contibute to $H_2$ formation. *Angew Chem Int Ed* 49(40):7350–7352.
15. Hornekaer L, et al. (2006) Metastable structures and recombination pathways for atomic hydrogen on the graphite (0001) surface. *Phys Rev Lett* 96(15):156104.
16. Hornekaer L, et al. (2006) Clustering of chemisorbed H(D) atoms on the graphite (0001) surface due to preferential sticking. *Phys Rev Lett* 97(18):186102.
17. Andree A, Le Lay M, Zecho T, Küppers J (2006) Pair formation and clustering of D on the basal plane of graphite. *Chem Phys Lett* 425(1–3):99–104.
18. Casolo S, Løvvik OM, Martinazzo R, Tantardini GF (2009) Understanding adsorption of hydrogen atoms on graphene. *J Chem Phys* 130(5):054704.
19. Rogeau N, Teillet-Billy D, Sidis V (2006) Double H atom adsorpition on a cluster model of a graphite surface. *Chem Phys Lett* 431(1–3):135–138.
20. Casolo S, Martinazzo R, Bonfanti M, Tantardini GF (2009) Quantum dynamics of the Eley-Rideal hydrogen formation reaction on graphite at typical interstellar cloud conditions. *J Phys Chem A* 113(52):14545–14553.
21. Sha X, Jackson B, Lemoine D (2002) Quantum studies of Eley-Rideal reactions between H atoms on a graphite surface. *J Chem Phys* 116(16):7158–7169.
22. Martinazzo R, Tantardini GF (2006) Quantum study of Eley-Rideal reaction and collision induced desorption of hydrogen atoms on a graphite surface. I. H-chemisorbed case. *J Chem Phys* 124(12):124702.
23. Thomas C, Angot T, Layet J-M (2008) Investigation of D(H) abstraction by means of HR-EELS. *Surf Sci* 602(13):2311–2314.
24. Aréou E, Cartry G, Layet J-M, Angot T (2011) Hydrogen-graphite interaction: Experimental evidences of an adsorption barrier. *J Chem Phys* 134(1):014701.
25. Zecho T, et al. (2002) Abstraction of D chemisorbed on graphite (0001) with gaseous H atoms. *Chem Phys Lett* 366(1–2):188–195.
26. Kammler T, Kolovos-Vellianitis D, Küppers J (2000) A hot-atom reaction model for H abstraction from solid surfaces. *Surf Sci* 460(1–3):91–100.
27. Creighan SC, Perry JS, Price SD (2006) The rovibrational distribution of $H_2$ and HD formed on a graphite surface at 15-50 K. *J Chem Phys* 124(11):114701.
28. Islam F, Latimer ER, Price SD (2007) The formation of vibrationally excited HD from atomic recombination on cold graphite surfaces. *J Chem Phys* 127(6):064701.
29. Latimer ER, Islam F, Price SD (2008) Studies of HD formed in excited vibrational states from atomic recombination on cold graphite surfaces. *Chem Phys Lett* 455(4–6): 174–177.
30. Morisset S, Aguillon F, Sizun M, Sidis V (2004) Quantum dynamics of $H_2$ formation on a graphite surface through the Langmuir Hinshelwood mechanism. *J Chem Phys* 121(13):6493–6501.
31. Morisset S, Aguillon F, Sizun M, Sidis V (2005) Wave-packet study of $H_2$ formation on a graphite surface through the Langmuir-Hinshelwood mechanism. *J Chem Phys* 122(19):194702.
32. Bachellerie D, Sizun M, Aguillon F, Sidis V (2009) Effects of a nonrigid graphene surface on the LH associative desorption of H atoms and on the deexcitation of nascent $H_2$ molecules colliding with model walls of carbonaceous porous material. *J Phys Chem A* 113(1):108–117.
33. Jackson B, Lemoine D (2001) Eley-Rideal reactions between H atoms on metal and graphite surfaces: The variation of reactivity with substrate. *J Chem Phys* 144(1): 474–482.
34. Gavardi E, Cuppen HM, Hornekær L (2009) A kinetic Monte Carlo study of desorption of $H_2$ from graphite (0001). *Chem Phys Lett* 477(4–6):285–289.
35. Jura M (1975) Interstellar clouds containing optically thick $H_2$. *Astrophys J* 197: 581–586.
36. Gry C, et al. (2002) $H_2$ formation and excitation in the interstellar medium. *Astron Astrophys* 391(2):675–680.
37. Lepetit B, Lemoine D, Medina Z, Jackson B (2011) Sticking and desorption of hydrogen on graphite: A comparative study of different models. *J Chem Phys* 134(11): 114705.
38. Bonfanti M, Casolo S, Tantardini GF, Ponti A, Martinazzo R (2011) A few simple rules governing hydrogenation of graphene dots. *J Chem Phys* 135(16):164701.
39. Kresse G, Hafner J (1994) Ab initio molecular-dynamics simulation of the liquid-metal-amorphous-semiconductor transition in germanium. *Phys Rev B Condens Matter* 49(20):14251–14269.
40. Perdew JP, et al. (1992) Atoms, molecules, solids, and surfaces: Applications of the generalized gradient approximation for exchange and correlation. *Phys Rev B Condens Matter* 46(11):6671–6687.
41. Vanderbilt D (1990) Soft self-consistent pseudopotentials in a generalized eigenvalue formalism. *Phys Rev B Condens Matter* 41(11):7892–7895.
42. Martinazzo R, Tantardini GF (2006) Quantum study of Eley-Rideal reaction and collision induced desorption of hydrogen atoms on a graphite surface. II. H-physisorbed case. *J Chem Phys* 124(12):124703.
43. Colbert DT, Miller WH (1992) A novel discrete variable representation for quantum mechanical reactive scattering via the S-matrix Kohn method. *J Chem Phys* 96(3): 1982–1991.